ACS APPLIED MATERIALS & INTERFACES

Research Article

www.acsami.org

Prediction of Stable Ruthenium Silicides from First-Principles Calculations: Stoichiometries, Crystal Structures, and Physical Properties

Chuanzhao Zhang,[†] Xiaoyu Kuang,[*,†] Yuanyuan Jin,[†] Cheng Lu,[*,‡,¶] Dawei Zhou,[‡] Peifang Li,[§] Gang Bao,[§] and Andreas Hermann[*,∥]

[†]Institute of Atomic and Molecular Physics, Sichuan University, Chengdu 610065, China

[‡]Department of Physics, Nanyang Normal University, Nanyang 473061, China

[¶]Beijing Computational Science Research Center, Beijing 100084, China

[§]College of Physics and Electronic Information, Inner Mongolia University for the Nationalities, Tongliao 028043, China

[∥]Centre for Science at Extreme Conditions and SUPA, School of Physics and Astronomy, The University of Edinburgh, Edinburgh EH9 3JZ, United Kingdom

Supporting Information

ABSTRACT: We present results of an unbiased structure search for stable ruthenium silicide compounds with various stoichiometries, using a recently developed technique that combines particle swarm optimization algorithms with first-principles calculations. Two experimentally observed structures of ruthenium silicides, RuSi (space group $P2_13$) and Ru_2Si_3 (space group *Pbcn*), are successfully reproduced under ambient pressure conditions. In addition, a stable $RuSi_2$ compound with β-$FeSi_2$ structure type (space group *Cmca*) was found. The calculations of the formation enthalpy, elastic constants, and phonon dispersions demonstrate the *Cmca*-$RuSi_2$ compound is energetically, mechanically, and dynamically stable. The analysis of electronic band structures and densities of state reveals that the *Cmca*-$RuSi_2$ phase is a semiconductor with a direct band gap of 0.480 eV and is stabilized by strong covalent bonding between Ru and neighboring Si atoms. On the basis of the Mulliken overlap population analysis, the Vickers hardness of the *Cmca* structure $RuSi_2$ is estimated to be 28.0 GPa, indicating its ultra-incompressible nature.

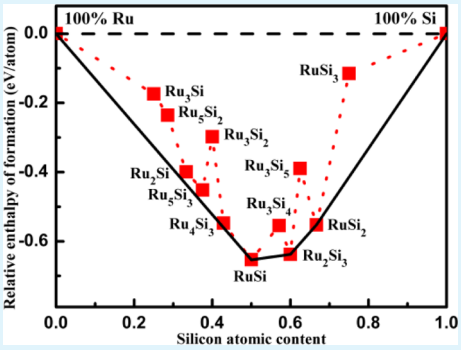

KEYWORDS: *ruthenium silicides, stoichiometries, crystal structures, mechanical properties, electronic structures, hardness*

INTRODUCTION

Transition-metal silicides have been studied theoretically and experimentally for a long time.[1−8] The study of their metallographic and electronic structures is particularly interesting, as they can exhibit novel physical properties such as high thermal stability, good conductivity, and low chemical reactivity.[3,4,6,7] Their stability and oxidation resistance make these silicides excellent high-temperature structural materials, for instance, for advanced aerospace applications.[5,6] Their relatively low electrical resistance has been utilized in microelectronics for the development of integrated circuit technology and design of microelectronic devices.[7] Until now, some 3d transition metal silicides,[3,4,6,7] such as CrSi and MnSi, have been studied in detail, both theoretically and experimentally, whereas data on the 4d transition metal silicides is quite limited, and some problems are still unresolved, especially for ruthenium silicides.

The ruthenium silicides are probably the technologically most important binary system among the 4d transition metal silicide alloys. The silicides in the Ru−Si binary system are promising new optoelectronic and thermoelectric materials, for instance, as light-emitting diodes,[9,10] infrared detectors,[11] and electro-optic interconnects.[11] According to the Ru−Si phase diagram,[12] ruthenium and silicon form several intermetallic compounds such as RuSi, Ru_2Si, Ru_2Si_3, and Ru_4Si_3. RuSi, an analogue of FeSi, is known to exist in two polymorphic forms, one having the FeSi-type structure at low temperatures and the other possessing the CsCl-type structure at high temperatures. Buschinger et al.[13] reported that a phase transition between the two structures occurs at 1578 K, while the transition temperature is strongly decreasing with increasing Ru excess. Kuntz et al.[14] determined the molar heat capacities of RuSi and Ru_2Si_3 by differential scanning calorimetry in the temperature range from 310 to 1080 K. The compounds Ru_4Si_3, RuSi, and Ru_2Si_3 have been studied by Perring et al.[15] using X-ray diffraction and electron probe microanalysis. Similarly, the enthalpies of formation for the three ruthenium−silicon compounds have been determined. The compound Ru_5Si_3,

Received: September 17, 2015
Accepted: November 18, 2015
Published: November 18, 2015

ACS Publications © 2015 American Chemical Society

DOI: 10.1021/acsami.5b08807
ACS Appl. Mater. Interfaces 2015, 7, 26776−26782

Table 1. Structural Parameters *a*, *b*, and *c*, Cell Volume per Formula Unit (V), Total Energies per Atom E, and Formation Enthalpies per Atom ΔH for the Phases with the Least Formation Enthalpy of Each Components of Ru−Si System, Compared with Experimental and Theoretical Data

	space group	*a* (Å)	*b* (Å)	*c* (Å)	V (Å^3)	E (eV)	ΔH (eV)
Ru_3Si	$I4/mcm$	5.394	5.394	5.394	108.079	−1978.74	−0.174
Ru_5Si_2	$P6_3cm$	7.099	7.099	12.975	566.245	−1889.69	−0.235
Ru_2Si	$Pnma$	5.295	4.017	7.447	158.390	−1771.05	−0.399
		5.287[a]	4.005[a]	7.413[a]	156.966[a]		
Ru_5Si_3	$Pbam$	5.269	9.843	4.036	209.318	−1667.15	−0.452
Ru_3Si_2	$Cmc2_1$	8.756	8.756	7.280	554.659	−1604.62	−0.298
Ru_4Si_3	$Pnma$	5.215	4.021	17.266	362.002	−1533.58	−0.548
		5.187[a]	4.021[a]	17.128[a]	357.237[a]		
RuSi	$P2_13$	4.727	4.727	4.727	105.629	−1355.47	−0.653
		4.750[b]	4.750[b]	4.750[b]	107.138[b]		
		4.701[c]	4.701[c]	4.701[c]	103.863[c]		
Ru_3Si_4	$Pnma$	19.935	3.016	6.218	388.946	−1177.16	−0.554
Ru_2Si_3	$Pbcn$	11.114	8.990	5.555	555.022	−1105.96	−0.637
		11.052[a]	8.937[a]	5.525[a]	545.714[a]		
		11.057[d]	8.934[d]	5.538[d]	547.060[d]		
$RuSi_2$	$Cmca$	10.168	8.107	8.209	676.650	−939.54	−0.552
		10.223[e]	8.133[e]	8.250[e]	685.935[e]		
$RuSi_3$	$Pnma$	14.927	2.883	5.926	255.048	−731.19	−0.115

[a]Reference 15. [b]Reference 36. [c]Reference 37. [d]Reference 11. [e]Reference 20.

with space group *Pbam* structure, which has been identified by Engstrom[16] and Weitzer et al.,[17] has not been confirmed in the redetermination of the phase diagram by Perring et al.[15] This discrepancy is most probably due to analytical problems, and more specifically to the matrix-effect correction procedure, as its amplitude is tightly related to the stoichiometry of the compound. It is therefore one objective here to determine whether such stoichiometry exists or not.

More recently, experimental and computational evidence was provided for a new silicon-rich phase, $RuSi_2$. The structure was not resolved in experiment, and density functional calculations considered three structure types found in the $FeSi_2$ analogue.[18−20] Lately, high-throughput electronic structure calculations on transition metal silicides, restricted to known structure types, also found $RuSi_2$ to be stable, in the orthorhombic β-$FeSi_2$ structure of *Cmca* symmetry.[21] No independent search for potential $RuSi_2$ structures beyond known structure types has been performed to date, and analyses have been restricted to the electronic structure. The goal of this work is to address this deficiency and provide an exemplary case study of transition metal silicides.

To find stable Ru−Si compounds that include structures that may not have been previously observed experimentally or computationally, we performed here a systematic study on binary ruthenium silicides using the Crystal Structure Analysis by Particle Swarm Optimization (CALYPSO) method in conjunction with first-principles calculations. Following CALYPSO structure searches, we selected structures on the convex hull, or close to it, and relaxed them. These calculations confirmed the stability of three stoichiometries—recently suggested $RuSi_2$ as well as previously known RuSi and Ru_2Si_3. For these compounds, we also computed their mechanical and electronic properties. Meanwhile, we also confirmed the Ru_5Si_3 compound is not energetically stable in the ground state and at atmospheric pressure.

COMPUTATIONAL METHODS

The structure searches in the Ru−Si binary system at atmospheric pressure are based on the particle swarm optimization algorithm in conjunction with ab initio total energy calculations as implemented in CALYPSO code,[22−28] which requires only the chemical compositions under the given conditions. Our structural searches with system sizes containing one to four formula units (f.u.) per simulation cell were performed for stoichiometries Ru_mSi_n spanning from Ru_3Si to $RuSi_3$. In each search, the first generation of structures is produced randomly and subsequently optimized. Each generation contains 30 structures. For the next generation, 60% of the structures are generated from the lowest-enthalpy structures provided by the previous generation, evolved using particle swarm optimization, while 40% will be generated randomly. We usually followed 50 generations to achieve convergence of the sampling of the low-energy minima in configurational space. Next, among the 1000−1500 structures, the top 50 low-lying structures are collected as candidates for the lowest-energy structure. Those structures with energy difference from the lowest-lying structures less than 0.5 eV (usually ∼20) are further optimized to identify the lowest-energy structure.

All structural relaxations and electronic structure calculations were performed using density functional theory within the Perdew−Burke−Ernzerhof (PBE) generalized gradient approximation functionals,[29] as implemented in the CASTEP code.[30] The ultrasoft pseudopotentials treat $4d^75s^1$ and $3s^23p^2$ as the valence electrons for the Ru and Si atoms, respectively. A cutoff energy of 500 eV for the expansion of the wave function into plane waves and appropriate Monkhorst−Pack k meshes were chosen to ensure that enthalpy calculations were well-converged to better than 1 meV/atom.[31] During the structural optimization, all atoms were fully relaxed using the conjugate gradient method until the total energy changes, force, and atomic displacement were less than 5.0×10^{-6} eV/atom, 0.01 eV/Å, and 0.0005 Å, respectively. The phonon dispersion calculations were performed by using a supercell approach as implemented in the PHONOPY code.[32,33]

RESULTS AND DISCUSSION

In the first instance, structure searches were performed using one to six formula units of ruthenium and silicon at atmospheric pressure. Noticeably, our structure searches succeed in finding the well-known hexagonal $P6_3/mmc$

DOI: 10.1021/acsami.5b08807
ACS Appl. Mater. Interfaces 2015, 7, 26776−26782

structure of Ru and cubic $Fd\bar{3}m$ structure of Si observed in experiments under ambient conditions,[34,35] thus providing important support for the reliability of the present structure searches. Table 1 summarizes the formation enthalpies of the binary Ru−Si system. The formation enthalpies were calculated as $\Delta H = [E(\mathrm{Ru}_m\mathrm{Si}_n) - mE(\text{Solid Ru}) - nE(\text{Solid Si})]/(m+n)$. ΔH is then the relative formation enthalpy per atom of a compound of this stoichiometry, $E(\mathrm{Ru}_m\mathrm{Si}_n)$ is the total energy/formula unit of the compound, E(Solid Ru) and E(Solid Si) are the equilibrium energies of pure Ru and Si at the ground state[34,35] (using their hexagonal $P6_3/mmc$ and cubic $Fd\bar{3}m$ phases, respectively), and m and n are the number of Ru and Si atoms for a system, respectively. Uncertainties in ΔH should be dominated by the density functional theory error (i.e., the approximation of the exchange-correlation energy). However, the PBE functional can describe the types of metallic and covalent bonding seen in the Ru−Si compounds very well and should thus provide reliable values for ΔH across the binary phase diagram. A compound is stable if it satisfies three prerequisites: (1) a lower enthalpy than any isochemical mixture of the elements or other compounds, that is, negative formation enthalpy; (2) thermodynamic stability when competing with its two nearest neighboring compositions; and (3) mechanical and dynamic stability via elastic constants and phonon dispersions.

Conditions (1) and (2) can be summarized quite concisely in so-called convex hull (or tieline, or global stability line) plots. Therefore, we plot $\Delta H(\mathrm{Ru}_m\mathrm{Si}_n)$ as defined above versus the mixing ratio (or, in this case, the silicon content) $n/(m+n)$. The convex hull of these points then connects the phases with the lowest formation enthalpies among all compositions, and any phases lying exactly on the convex hull are deemed as energetically stable, both against decomposition into the elements and into any combination of other binary compounds. Of course, structures whose enthalpies remain above the convex hull would be thermodynamically metastable and perhaps can be synthesized under particular conditions. The convex hull for the Ru−Si system at atmospheric pressure is shown in Figure 1. From Figure 1, it can clearly be seen that

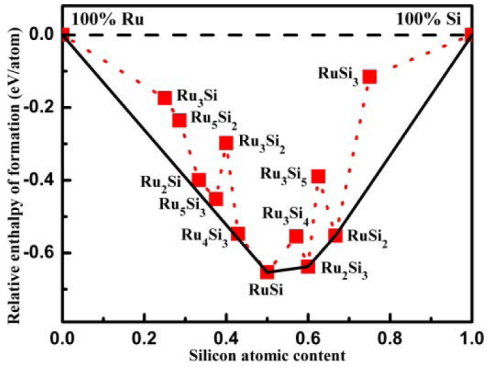

Figure 1. Convex hull of the Ru−Si system at atmospheric pressure. The solid line denotes the ground-state convex hull.

three compositions are stable: RuSi, Ru_2Si_3, and $RuSi_2$. The detailed structural parameters of the predicted phases of $\mathrm{Ru}_m\mathrm{Si}_n$ are listed in Tables S1 and S2 of the Supporting Information.

In good agreement with the experimental findings, our theoretical calculations reproduced successfully the experimentally observed structures and compositions for both RuSi (Figure 2a) and Ru_2Si_3 (Figure 2b).[15] RuSi is found to

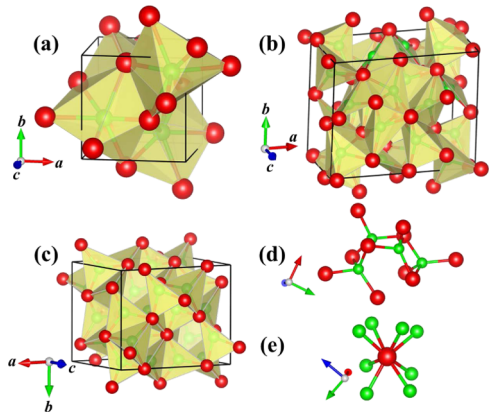

Figure 2. Crystal structures of (a) $P2_13$-RuSi, (b) $Pbcn$-Ru_2Si_3, and (c) $Cmca$-$RuSi_2$. (d, e) The coordination environment of Si and Ru, respectively. The red and green spheres represent ruthenium and silicon atoms, respectively, and $SiRu_n$ polyhedra are shaded in all phases.

crystallize in the cubic $P2_13$ ground-state phase with a formation enthalpy of 23 meV per atom lower than the $Pm\bar{3}m$ phase. Ru_2Si_3 has an orthorhombic $Pbcn$ ground state, which is lower, by 21 meV, than that of the $P\bar{4}c2$ phase. Spin-polarized calculations further revealed that both the RuSi and Ru_2Si_3 compounds are nonmagnetic. Noticeably, we find another compound that is more Si-rich than RuSi and Ru_2Si_3. $RuSi_2$ crystallizes in the $FeSi_2$ structure type, in an orthorhombic $Cmca$ structure (Figure 2c). The unit cell is composed of 48 atoms. Si atoms take the Wyckoff 16g positions (0.372, 0.277, 0.443) and (0.127, 0.051, 0.276). Ru atoms occupy two nonequivalent sites in this structure, the Wyckoff 8d (0.215, 0, 0) and 8f (0, 0.188, 0.818) positions. The structure consists of a three-dimensional network of edge-sharing distorted $SiRu_4$ tetrahedra (see Figure 2d). Conversely, Ru atoms are coordinated to eight Si atoms, forming a caged distorted tetragonal prism (Figure 2e). The shortest bond length of 2.452 Å is marginally larger than the sum of the covalent radii of Ru (r = 1.25 Å) and Si (r = 1.11 Å), indicating covalent bonding contributions. Additionally, we also succeeded in finding another composition, Ru_5Si_3 with space group $Pbam$, at 38 meV per atom above the convex hull and thus metastable, which explains why the Ru_5Si_3 compound was not observed in the differential thermal analysis, X-ray diffraction, and electron microprobe investigations by Perring et al.[15]

To verify the mechanical stability of the three ruthenium silicides, we calculated the elastic constants of RuSi ($P2_13$), Ru_2Si_3 ($Pbcn$), and $RuSi_2$ ($Cmca$), using the strain−stress method.[38] The full elastic stiffness constants of the three phases are given in Table S3 of the Supporting Information. It can be seen from Table S3 that all three ruthenium silicides fulfill their respective mechanical stability criteria.[39] The value of C_{22} for the $Cmca$ structure of $RuSi_2$ is larger than C_{11} and C_{33}, revealing that this polymorph is more difficult to be compressed along the b-axis than the a- and c-axes. The stability of the three ruthenium silicides is also confirmed through the calculations of the phonon dispersion curves, as there are no imaginary phonon frequencies detected in the whole Brillouin zone, see Figure 3.

Figure 4 shows electronic densities of states, both total (TDOS) and projected (PDOS) onto atomic orbitals, for the three stable ruthenium silicides (RuSi, Ru_2Si_3, and $RuSi_2$). It

DOI: 10.1021/acsami.5b08807
ACS Appl. Mater. Interfaces 2015, 7, 26776−26782

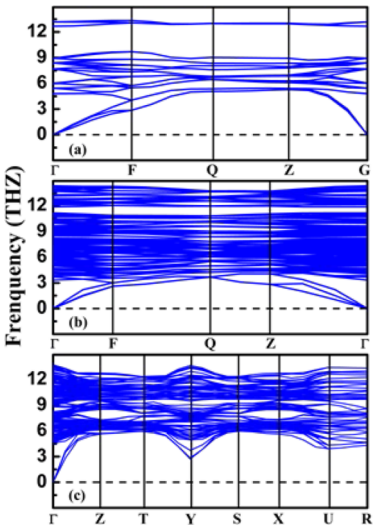

Figure 3. Phonon dispersions for (a) $P2_13$-RuSi, (b) *Pbcn*-Ru_2Si_3, and (c) *Cmca*-$RuSi_2$.

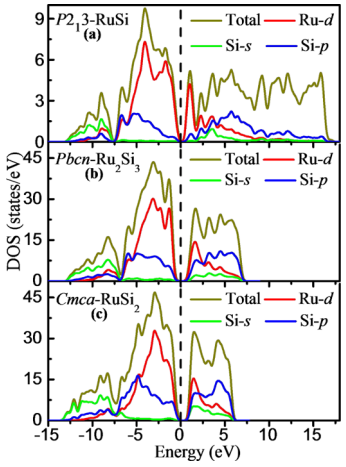

Figure 4. Total and partial densities of (a) $P2_13$-RuSi, (b) *Pbcn*-Ru_2Si_3, and (c) *Cmca*-$RuSi_2$.

can be seen clearly that the three compounds are semiconducting. This is corroborated by the electronic band structures, shown in Figure 5. The fundamental band gaps (indirect in $P2_13$-RuSi and direct in *Pbcn*-Ru_2Si_3 and *Cmca*-$RuSi_2$) are 0.275, 0.564, and 0.48 eV, respectively, which is in good agreement with the experimental measurements and relevant theoretical calculations.[11,21,40−47] The TDOS and PDOS can be divided into three regions. First, in the low-energy region of −13.0 to ca. −7.0 eV, the TDOS is dominated by the Si-3s state. Second, in the region of the valence band (from −7.0 eV to the valence band maximum) the TDOS originates from mixing of Ru-4d and Si-3p states. Finally, the conduction band (below 6.5 eV) is dominated by unoccupied Si-3p and Ru-4d states. It is worth mentioning that the significant hybridization effects between Si-3p and Ru-4d states on either side of the band gap indicate that strong Ru−Si covalent bonding exists in all stable Ru−Si compounds. Interestingly, there is a strong peak at −2.43 eV for the *Cmca* structure of $RuSi_2$, indicating a stronger localization of 4d electrons than the other, more Ru-rich phases. The strong covalent bonding between Ru and neighboring Si atoms can also be be seen from the electron localized function (ELF), as

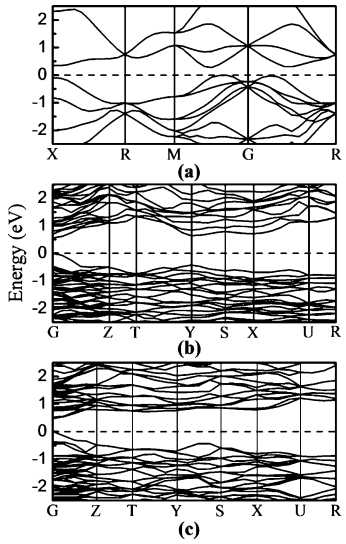

Figure 5. Band structures for (a) $P2_13$-RuSi, (b) *Pbcn*-Ru_2Si_3, and (c) *Cmca*-$RuSi_2$.

shown in Figure 6. ELF reaches maxima of 0.800 along the nearest-neighbor Ru−Si connections.

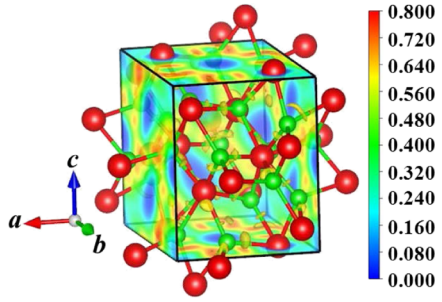

Figure 6. ELF maps of the *Cmca*-$RuSi_2$ phase.

On the basis of the large shear modulus G and the small values for the B/G ratio and Poission's ratio ν (see Table S3), as well as the strong covalent bonding, the $RuSi_2$ (*Cmca*) phase can be considered as a potential semiconductor material with high hardness. We now explore further the hardness for the three ruthenium silicides using the microscopic hardness model proposed by Gao et al.[48,49] The Vickers hardness of complex crystals can be calculated by the following formula:

$$H_v = [\prod^{\mu} (699P^{\mu}(\nu_b^{\mu})^{-5/3})^{n^{\mu}}]^{1/\Sigma n^{\mu}} \quad (1)$$

where

$$\nu_b^{\mu} = (d^{\mu})^3/\Sigma[(d^{\nu})^3 N_b^{\nu}] \quad (2)$$

where μ labels all different types of covalent bonds in the system, P^{μ} is the Mulliken overlap population of the μ type bond, ν_b^{μ} is its volume, n^{μ} is the number of μ type bonds, d^{μ} is its bond length, and N_b^{ν} is the bond number of type μ per unit volume. Using the above simple empirical hardness formula, the Vickers hardness of the three ruthenium silicides was calculated. The calculated results are summarized in Table 2. To benchmark our hardness calculations, we compare the calculated hardness value of Si with the experimental result.[50] The predicted hardness of silicon is in good agreement with the experimental value. According to our calculations, the hardness

DOI: 10.1021/acsami.5b08807
ACS Appl. Mater. Interfaces 2015, 7, 26776−26782

Table 2. Calculated Bond Parameters and Vickers Hardness H_v (GPa) for Three Ground-State Structures

	bond	n	d (Å)	P	ν_b (Å^3)	H_v (GPa)
$Fd\bar{3}m$	Si−Si	16	2.365	0.73	10.194	10.6
-Si						11.3[a]
$P2_13$	Ru−Si	4	2.385	0.13	2.706	12.6
-RuSi		12	2.426	0.47	2.850	
	Si−Si	12	2.936	0.05	5.501	
Pbcn	Ru−Si	8	2.328	0.64	2.809	19.2
-Ru_2Si_3		8	2.363	0.25	2.939	
		8	2.377	0.53	2.993	
		8	2.387	0.54	3.029	
		8	2.412	0.29	3.128	
		8	2.415	0.58	3.137	
		8	2.453	0.20	3.289	
		8	2.468	0.33	3.349	
		8	2.498	0.40	3.472	
		8	2.510	0.57	2.522	
		8	2.521	0.26	3.569	
		8	2.528	0.40	3.599	
		8	2.606	0.27	3.942	
	Si−Si	8	2.642	0.21	4.106	
		4	2.694	0.13	4.355	
		8	2.740	0.12	4.581	
		8	2.816	0.13	4.974	
		8	2.820	0.01	4.997	
		8	2.958	0.09	5.766	
Cmca	Ru−Si	16	2.452	0.38	3.081	28.0
-$RuSi_2$		16	2.459	0.35	3.109	
		16	2.460	0.41	3.112	
		16	2.460	0.30	3.113	
		16	2.466	0.36	3.138	
		16	2.484	0.31	3.204	
		16	2.500	0.30	3.269	
		16	2.522	0.27	3.354	
	Si−Si	8	2.540	0.33	3.425	
		16	2.568	0.32	3.542	
		8	2.579	0.28	3.587	
		8	2.594	0.28	3.651	
		16	2.613	0.31	3.730	
		8	2.694	0.18	4.087	
		16	2.694	0.20	4.088	

[a]Reference 50.

values of $P2_13$-RuSi, *Pbcn*-Ru_2Si_3, and *Cmca*-$RuSi_2$ crystals are 12.3, 19.2, and 28.0 GPa, respectively. This suggests that the hardness values increase with the increasing Si content, and all compounds are significantly harder than pure Si. Generally speaking, the origin of differences in hardness is related not only to the strengths of individual Si−Si and Ru−Si covalent bonds but also to the orientation of bonds, especially for bonds between layers. The difference in hardness between pure Si and the three compounds can be attributed not only to the Si concentration, but also to modifications in the chemical bonding between the Ru and Si atoms. With increasing Si concentration, the bond length of the Si−Si covalent bond decreases, while all along remaining longer than in pure Si. Thus, the trends in hardness in the three compounds are likely compounded by strong Ru−Si covalent interactions and modified Si−Si interactions. It is found that the hardness of the *Cmca* phase $RuSi_2$ approaches that of WC (30.0 GPa),[51] which suggests that the $RuSi_2$ compound is indeed a promising hard semiconducting material at ambient conditions.

CONCLUSION

In summary, using the particle swarm optimization algorithm in combination with first-principles electronic calculations, we explored the binary ruthenium silicide phase diagram. Under ambient conditions, a new potentially ultra-incompressible material of $RuSi_2$ with the space group of *Cmca* ($FeSi_2$ structure type) was discovered. The orthorhombic *Cmca* structure of $RuSi_2$ is mechanically and dynamically stable, as determined by calculating elastic constants and phonon dispersions, respectively. Additionally, the calculated electronic band structure and density of states suggest that $RuSi_2$ is a small-gap semiconductor. Our analyses show that its bonding nature can be described as covalent-like due to the hybridization of Si-3p and Ru-4d states, which is also verified by the electron localized function. Its Vickers hardness value based on the Mulliken overlap population analysis reaches 28.0 GPa, demonstrating the *Cmca*-$RuSi_2$ crystal is a semiconducting material with potential high hardness under atmospheric pressure. The current theoretical predictions will most likely promote further experimental and theoretical studies on the ruthenium silicides.

ASSOCIATED CONTENT

Supporting Information

The Supporting Information is available free of charge on the ACS Publications website at DOI: 10.1021/acsami.5b08807.

Details of crystal structures and mechanical properties of ruthenium silicides. Tabulated calculated structural parameters and Wyckoff sites. Calculated elastic constants, bulk modulus, shear modulus, Young's modulus. (PDF)

AUTHOR INFORMATION

Corresponding Authors

*E-mail: scu_kuang@163.com. (X.K.)
*E-mail: lucheng@calypso.cn. (C.L.)
*E-mail: a.hermann@ed.ac.uk. (A.H.)

Notes

The authors declare no competing financial interest.

ACKNOWLEDGMENTS

This work was supported by the National Natural Science Foundation of China (Nos. 11274235, 11304167, and 11304143), Henan Joint Funds of the National Natural Science Foundation of China (No. U1304612), Program for Science & Technology Innovation Talents in Universities of Henan Province (No. 15HASTIT020), and Natural Science Foundation of Inner Mongolia (No. 2013MS0807).

REFERENCES

(1) Choi, J.; Choi, S.; Kim, J.; Na, S.; Lee, H. J.; Lee, S. K.; Kim, H. Silicide Formation Process of Er Films with Ta and TaN Capping Layers. *ACS Appl. Mater. Interfaces* **2013**, *5*, 12744−12750.

(2) Dahal, N.; Wright, J. T.; Willey, T. M.; Meulenberg, R. W.; Chikan, V. Preparation of Iron and Gold Silicide Nanodomains on Silicon (111) by the Reaction of Gold, Iron-Gold Core-Shell, and Alloy Nanoparticles with Triethylsilane. *ACS Appl. Mater. Interfaces* **2010**, *2*, 2238−2274.

(3) Lin, Y. C.; Chen, Y.; Huang, Y. The Growth and Applications of Silicides for Nanoscale Devices. *Nanoscale* **2012**, *4*, 1412−1421.

DOI: 10.1021/acsami.5b08807
ACS Appl. Mater. Interfaces 2015, 7, 26776−26782

(4) Schmitt, A. L.; Higgins, J. M.; Szczech, J. R.; Jin, S. Synthesis and Applications of Metal Silicide Nanowires. *J. Mater. Chem.* **2010**, *20*, 223−235.
(5) Shao, G. Prediction of Structural Stabilities of Transition-metal Disilicide Alloys by the Density Functional Theory. *Acta Mater.* **2005**, *53*, 3729−3736.
(6) Wang, H.; Wu, J. C.; Shen, Y.; Li, G.; Zhang, Z.; Xing, G.; Guo, D.; Wang, D.; Dong, Z.; Wu, T. $CrSi_2$ Hexagonal Nanowebs. *J. Am. Chem. Soc.* **2010**, *132*, 15875−15877.
(7) Zhou, S.; Wang, D. Unique Lithiation and Delithiation Processes of Nanostructured Metal Silicides. *ACS Nano* **2010**, *4*, 7014−7020.
(8) Chen, Y.; Kolmogorov, A. N.; Pettifor, D. G.; Shang, J. X.; Zhang, Y. Theoretical Analysis of Structural Stability of TM_5Si_3 Transition Metal Silicides. *Phys. Rev. B: Condens. Matter Mater. Phys.* **2010**, *82*, 507.
(9) Lindholm, N.; Morse, M. D. Rotationally Resolved Spectra of Jet-cooled RuSi. *J. Chem. Phys.* **2007**, *127*, 084317.
(10) Zhao, Y. N.; Han, H. L.; Yu, Y.; Xue, W. H.; Gao, T. First-principles Studies of the Electronic and Dynamical Properties of Monosilicides MSi (M = Fe, Ru, Os). *Europhys. Lett.* **2009**, *85*, 47005.
(11) Wolf, W.; Bihlmayer, G.; Blügel, S. Electronic Structure of the Nowotny Chimney-ladder Silicide Ru_2Si_3. *Phys. Rev. B: Condens. Matter Mater. Phys.* **1997**, *55*, 6918−6926.
(12) Okamoto, H. Ru-Si (Ruthenium-Silicon). *J. Phase Equilib.* **2002**, *23*, 388.
(13) Buschinger, B.; Geibel, C.; Diehl, J.; Weiden, M.; Guth, W.; Wildbrett, A.; Horn, S.; Steglich, F. Preparation and Low Temperature Properties of FeSi-type RuSi. *J. Alloys Compd.* **1997**, *256*, 57−60.
(14) Kuntz, J. J.; Perring, L.; Feschotte, P.; Gachon, J. C. Heat Capacity and Heat Content Measurements on Binary Compounds in the Ru-Si, Ru-Ge, and Ru-Sn Systems. *J. Solid State Chem.* **1997**, *133*, 439−444.
(15) Perring, L.; Bussy, F.; Gachon, J. C.; Feschotte, P. The Ruthenium-Silicon System. *J. Alloys Compd.* **1999**, *284*, 198−205.
(16) Engström, I. Note on the Crystal Structures of Ru_5Si_3 and PdSi. *Acta Chem. Scand.* **1970**, *24*, 1466−1468.
(17) Weitzer, F.; Rogl, P.; Schuster, J. C. X-Ray Investigations in the Systems Ruthenium-Silicon and Ruthenium-Silicon-Nitrogen. *Z. Metallkd.* **1988**, *79*, 154−156.
(18) Ivanenko, L.; Behr, G.; Spinella, C. R.; Borisenko, V. E. $RuSi_2$: Evidence of a New Binary Phase in the Ruthenium-Silicon System. *J. Cryst. Growth* **2002**, *236*, 572−576.
(19) Ivanenko, L. I.; Shaposhnikov, V. L.; Filonov, A. B.; Krivosheeva, A. V.; Borisenko, V. E.; Migas, D. B.; Miglio, L.; Behr, G.; Schumann, J. Electronic Properties of Semiconducting Silicides: Fundamentals and Recent Predictions. *Thin Solid Films* **2004**, *461*, 141−147.
(20) Shaposhnikov, V. L.; Filonov, A. B.; Krivosheeva, A. V.; Ivanenko, L. I.; Borisenko, V. E. Structural, Electronic and Optical Properties of a New Binary Phase - Ruthenium Disilicide. *Phys. Status Solidi B* **2005**, *242*, 2864−2871.
(21) Opahle, I.; Madsen, G. K. H.; Drautz, R. High Throughput Density Functional Investigations of the Stability, Electronic Structure and Thermoelectric Properties of Binary Silicides. *Phys. Chem. Chem. Phys.* **2012**, *14*, 16197−16202.
(22) Wang, Y.; Lv, J.; Zhu, L.; Ma, Y. CALYPSO: A Method for Crystal Structure Prediction. *Comput. Phys. Commun.* **2012**, *183*, 2063−2070.
(23) Lv, J.; Wang, Y.; Zhu, L.; Ma, Y. Particle-swarm Structure Prediction on Clusters. *J. Chem. Phys.* **2012**, *137*, 084104.
(24) Wang, Y.; Lv, J.; Zhu, L.; Ma, Y. Crystal Structure Prediction via Particle-swarm Optimization. *Phys. Rev. B: Condens. Matter Mater. Phys.* **2010**, *82*, 094116.
(25) Wang, Y.; Miao, M.; Lv, J.; Zhu, L.; Yin, K.; Liu, H.; Ma, Y. An Effective Structure Prediction Method for Layered Materials Based on 2D Particle Swarm Optimization Algorithm. *J. Chem. Phys.* **2012**, *137*, 224108.
(26) Li, P.; Zhou, R.; Zeng, X. C. Computational Analysis of Stable Hard Structures in the Ti-B System. *ACS Appl. Mater. Interfaces* **2015**, *7*, 15607−15617.
(27) Zhu, L.; Liu, H.; Pickard, C. J.; Zou, G.; Ma, Y. Reactions of Xenon with Iron and Nickel are Predicted in the Earth's Inner Core. *Nat. Chem.* **2014**, *6*, 644−648.
(28) Lu, S.; Wang, Y.; Liu, H.; Miao, M.; Ma, Y. Self-assembled Ultrathin Nanotubes on Diamond (100) Surface. *Nat. Commun.* **2014**, *5*, 3666.
(29) Perdew, J. P.; Burke, K.; Ernzerhof, M. Generalized Gradient Approximation Made Simple. *Phys. Rev. Lett.* **1996**, *77*, 3865−3868.
(30) Segall, M. D.; Lindan, P. J. D.; Probert, M. J.; Pickard, C. J.; Hasnip, P. J.; Clark, S. J.; Payne, M. C. First-principles Simulation: Ideas, Illustrations and the CASTEP Code. *J. Phys.: Condens. Matter* **2002**, *14*, 2717−2744.
(31) Monkhorst, H. J.; Pack, J. D. Special Points for Brillouin-zone Integrations. *Phys. Rev. B* **1976**, *13*, 5188−5192.
(32) Parlinski, K.; Li, Z. Q.; Kawazoe, Y. First-principles Determination of the Soft Mode in Cubic ZrO_2. *Phys. Rev. Lett.* **1997**, *78*, 4063−4066.
(33) Togo, A.; Oba, F.; Tanaka, I. First-principles Calculations of the Ferroelastic Transition between Rutile-type and $CaCl_2$-type SiO_2 at High Pressures. *Phys. Rev. B: Condens. Matter Mater. Phys.* **2008**, *78*, 134106.
(34) Cynn, H.; Klepeis, J. E.; Yoo, C. S.; Young, D. A. Osmium has the Lowest Experimentally Determined Compressibility. *Phys. Rev. Lett.* **2002**, *88*, 135701.
(35) Shen, G.; Ikuta, D.; Sinogeikin, S.; Li, Q.; Zhang, Y.; Chen, C. Direct Observation of a Pressure-Induced Precursor Lattice in Silicon. *Phys. Rev. Lett.* **2012**, *109*, 205503.
(36) Göransson, K.; Engström, I.; Noläng, B. Structure Refinements for Some Platinum Metal Monosilicides. *J. Alloys Compd.* **1995**, *219*, 107−110.
(37) Shaposhnikov, V. L.; Migas, D. B.; Borisenko, V. E.; Dorozhkin, N. N. Features of the Band Structure for Semiconducting Iron, Ruthenium, and Osmium Monosilicides. *Semiconductors* **2009**, *43*, 142−144.
(38) Lu, C.; Kuang, X. Y.; Wang, S. J.; Zhao, Y. R.; Tan, X. M. Theoretical Investigation on the High-pressure Structural Transition and Thermodynamic Properties of Cadmium Oxide. *Europhys. Lett.* **2010**, *91*, 16002.
(39) Wu, Z.; Zhao, E.; Xiang, H.; Hao, X.; Liu, X.; Meng, J. Crystal Structures and Elastic Properties of Superhard IrN_2 and IrN_3 from First Principles. *Phys. Rev. B: Condens. Matter Mater. Phys.* **2007**, *76*, 054115.
(40) Migas, D. B.; Miglio, L.; Shaposhnikov, V. L.; Borisenko, V. E. Structural, Electronic and Optical Properties of Ru_2Si_3, Ru_2Ge_3, Os_2Si_3 and Os_2Ge_3. *Phys. Status Solidi B* **2002**, *231*, 171−180.
(41) Hohl, H.; Ramirez, A. P.; Goldmann, C.; Ernst, G.; Bucher, E. Transport Properties of RuSi, RuGe, OsSi, and Quasi-binary Alloys of These Compounds. *J. Alloys Compd.* **1998**, *278*, 39−43.
(42) Hernandez, J. A.; Vočadlo, L.; Wood, I. G. High Pressure Stability of the Monosilicides of Cobalt and the Platinum Group Elements. *J. Alloys Compd.* **2015**, *626*, 375−380.
(43) Opahle, I.; Parma, A.; McEniry, E. J.; Drautz, R.; Madsen, G. K. H. High-throughput Study of the Structural Stability and Thermoelectric Properties of Transition Metal Silicides. *New J. Phys.* **2013**, *15*, 105010.
(44) Gottlieb, U.; Laborde, O.; Rouault, A.; Madar, R. Resistivity of Ru_2Si_3 Single Crystals. *Appl. Surf. Sci.* **1993**, *73*, 243−245.
(45) Henrion, W.; Rebien, M.; Birdwell, A. G.; Antonov, V. N.; Jepsen, O. Optical Interband Spectra and Band Structure of Ru_2Si_3 and Ru_2Ge_3. *Thin Solid Films* **2000**, *364*, 171−176.
(46) Vining, C. B.; McCormack, J. A.; Zoltan, A.; Zoltan, L. D. A Promising New Thermoelectric Material: Ruthenium Silicide. In *Proceedings Eighth Symposium on Space Nuclear Power Systems,* Albuquerque, New Mexico, Jan 6-10, 1991; El-Genk, M., Hoover, M., Eds.; American Institute of Physics: New York, 1991; pp 458−463.
(47) Imai, Y.; Watanabe, A. Consideration of the Validity of the 14 Valence Electron Rule for Semiconducting Chimney-ladder Phase Compounds. *Intermetallics* **2005**, *13*, 233−241.

DOI: 10.1021/acsami.5b08807
ACS Appl. Mater. Interfaces 2015, 7, 26776−26782

(48) Gao, F. Theoretical Model of Intrinsic Hardness. *Phys. Rev. B: Condens. Matter Mater. Phys.* **2006**, *73*, 132104.
(49) Gao, F.; He, J.; Wu, E.; Liu, S.; Yu, D.; Li, D.; Zhang, S.; Tian, Y. Hardness of Covalent Crystals. *Phys. Rev. Lett.* **2003**, *91*, 015502.
(50) Lide, D. R. *Handbook of Chemistry and Physics,* 90th ed; Berger, L. I., Ed.; Chemical Rubber Company: Boca Raton, FL, 2010; Chapter 12, pp 80−92.
(51) Haines, J.; Léger, J. M.; Bocquillon, G. Synthesis and Design of Superhard Materials. *Annu. Rev. Mater. Res.* **2001**, *31*, 1−23.

DOI: 10.1021/acsami.5b08807
ACS Appl. Mater. Interfaces 2015, 7, 26776−26782